Journal of Materials Chemistry B

PAPER

View Article Online
View Journal | View Issue



Cite this: J. Mater. Chem. B, 2014, 2, 1988

# A thermally triggered *in situ* hydrogel from poly(acrylic acid-*co*-*N*-isopropylacrylamide) for controlled release of anti-glaucoma drugs†

Adhimoorthy Prasannan,‡[a] Hsieh-Chih Tsai,‡*[b] Yu-Shuan Chen[c] and Ging-Ho Hsiue*[ac]

Received 30th September 2013
Accepted 15th January 2014

DOI: 10.1039/c3tb21360a

www.rsc.org/MaterialsB

The purpose of this study was to develop and evaluate thermally responsive copolymers, which contain temperature- and pH-sensitive segments that are either alternating in or grafted onto the main chain, and to exploit their temperature-sensitive properties for ophthalmic drug delivery. Accordingly, two types of thermoresponsive copolymers—a linear poly(acrylic acid-*co*-*N*-isopropylacrylamide) random copolymer (PAAc-*co*-PNIPAAm) and a poly(acrylic acid-*g*-*N*-isopropylacrylamide) graft copolymer (PAAc-*g*-PNIPAAm)—were investigated for their thermosensitive *in situ* gel formation and potential applications for ophthalmic drug delivery. All the PAAc-*g*-PNIPAAm graft copolymers, and the linear PAAc-*co*-PNIPAAm copolymer with low acrylic acid contents, have an LCST of 34 °C; this is close to the surface temperature of the eye and can therefore be utilized for ophthalmic drug delivery. In addition, the PAAc-*g*-PNIPAAm graft copolymers showed a higher water content than the linear random copolymer; this is due to the high water adsorption ability of PAAc. The drug release dynamics of [$^3$H]-epinephrine as a model showed that the linear random copolymer has a faster drug release, while the graft copolymers showed a more sustained release profile. The Ritger–Peppas model was used to account for the release of the epinephrine diffusion exponent '*n*' which was in between 0.5 and 0.6. The release of the drug is considered mainly dependent on diffusion but other factors cannot be excluded. We suspected that the dynamics of drug release are determined by the water adsorption ability because high water content results in the formation of a larger capillary network in the polymer matrix, which promotes drug diffusion into the copolymer. The results suggest that PAAc-*g*-PNIPAAm graft copolymers are potential thermosensitive *in situ* gel-forming materials for ophthalmic drug delivery.

## Introduction

Currently, ophthalmic diseases are a major health concern worldwide.[1] Ophthalmic drugs, such as glaucoma delivery systems, are usually in the form of conventional eye drops.[2] However, sometimes this mode of therapy is ineffective due to a limited amount (~5%) of the drug being absorbed into the targeted site and the remainder of the drug being absorbed in the conjunctiva and transnasal, which may cause side effects. Hence, further development is required to overcome drawbacks such as eye blinking side effects and drainage losses. Therefore, it is essential to establish novel delivery systems to improve the therapeutic effectiveness and reduce the unwanted side effects of eye blinking and drainage losses to achieve safe pharmaceuticals. Recent reports suggest that *in situ* gel formation by smart polymeric materials may be employed in controlled drug delivery.[3,4] In such smart polymeric materials, macro-morphological changes are induced in response to environmental alterations in the temperature, pH, ionic strength, *etc.*[5] Similarly, micro-conformational changes can be effected by light or by changes in the surrounding electromagnetic environment for physical signal-sensitive materials.[6] Therefore, the development of precise synthesis methods for smart polymeric materials is a rapidly growing area of polymer science and holds great promise for various applications in novel drug delivery and controlled release.[7–12] In particular, thermosensitive polymeric materials have successfully been used to increase the residence time of drug molecules and enable their controlled release for eye diseases owing to the improved bio-adhesiveness of the ophthalmic solutions, which is evident from their lower critical solution

[a]Department of Chemical Engineering/R&D Center for Membrane Technology, Chung Yuan University, Chung Li 320, Taiwan. E-mail: ghhsiue@mx.nthu.edu.tw; Fax: +886-3-5726825; Tel: +886-3-5719956

[b]Graduate Institute of Applied Science and Technology, National Taiwan University of Science and Technology, Taipei 106, Taiwan. E-mail: h.c.tsai@mail.ntust.edu.tw; Fax: +886-2-27303733; Tel: +886-2-27303625

[c]Department of Chemical Engineering, National Tsing Hua University, Hsinchu 320, Taiwan

† Electronic supplementary information (ESI) available. See DOI: 10.1039/c3tb21360a

‡ These authors contributed equally.

temperature (LCST) in water.[13,14] Poly(*N*-isopropylacrylamide) (PNIPAAm) is one of the most extensively studied thermosensitive polymers in various fields due to its distinct advantages of reversible surface properties and mild switching conditions.[15] Moreover, its LCST is 32 °C, which is close to body temperature and can be controlled by copolymerization with hydrophilic or hydrophobic monomers.[16]

To provide more versatile properties, such as higher water content, uniform film formation, and bioavailability, the incorporation into PNIPAAm of other functional comonomers[17,18] that contain ionizable groups may accelerate the phase transition when heated through the LCST or exposed to a range of stimuli based on the physiological pH range (1.2 to 7.4).[19] Poly(acrylic acid) (PAAc), which has ionizable groups, is a promising option due to its hydrophilicity, high swelling capacity, and good biocompatibility.[20] PAAc-based hydrogels are considered to be anionic, mucoadhesive polymers and are widely used in ophthalmic formulations due to their ionizable carboxylic groups that enable interactions with oppositely charged drugs during the formation of polymer–drug complexes.[21] This complex formation can impart controlled drug delivery and increased compatibility of the polymer and the drug. However, due to their high viscosity, PAAc hydrogels can cause blurred vision, crystal formation on the lids and lashes, and irritation.[22] Grafting poly(acrylic acid) onto a PNIPAAm-based thermoresponsive polymer may overcome these drawbacks.

PNIPAAm-based polymers and hydrogels have been studied in a number of diverse applications including recovery of solute, bioseparations, chromatography and tissue engineering.[23] PNIPAAm-based polymers have also been examined in drug delivery applications, especially ocular drug delivery by combination with cells. Significant research has been focused on using thermoresponsive hydrogels to deliver drugs for ocular diseases.[24–26] Our previous study demonstrated that PNIPAAm-containing epinephrine was more efficient than conventional eye drops; however, the PNIPAAm formed a rigid film and became uncomfortable after coming into contact with the cornea.[13] Hence, improving the hydrophilicity of the network may enhance the flexibility of the polymer. In this regard, Turturro *et al.* investigated poly(ethylene glycol) diacrylate (PEGDA) cross-linked with PNIPAAm hydrogels, which are good candidates for ocular drug delivery systems due to their thermal sensitivity and sustained-release characteristics; however, retinal parameters that indicate that transient effects persist after injection were found.[26] Cao *et al.* developed an *in situ* gelling system with timolol maleate and chitosan-grafted PNIPAAm as an injectable copolymer hydrogel (PNIPAAm–CS) and compared it with conventional eye drops.[27]

For glaucoma treatment, there are several drugs that are commonly used, which belong to different pharmacological classes, including parasympathomimetics (pilocarpine, carbachol), sympathomimetics (adrenaline, epinephrine), carbonic anhydrase inhibitors (acetazolamide, dorzolamide), β-adrenergic receptor antagonists (carteolol, timolol), and so on.[28] Most of these drugs are administered as eye drops and follow an intra-ocular pressure (IOP) reducing mechanism. In particular, sympathomimetics such as epinephrine have been the forerunner in anti-glaucoma therapy for about a century due to their capability to reduce aqueous humor and increase its outflow. Additionally, they can induce vasoconstriction of the conjunctival vessels on the ocular surface and their IOP reducing capacity. There is a lack of research focused on the mucoadhesive properties of PAAc in thermoresponsive hydrogels for sympathomimetic-based drug delivery to treat ocular diseases.

Herein, we report the synthesis of PAAc-*co*-PNIPAAm-based random and graft copolymers by free radical polymerization and investigate the effects of the polymerization method on the polymer properties. The resulting polymer networks were used for ophthalmic drug delivery of a model drug. The structures, water content, and LCST behavior of the different polymers were characterized, and their capacities for sustained ophthalmic-drug release were investigated. The use of these copolymer hydrogels may be promising for the treatment of ophthalmic diseases through the extended release of hydrophilic ocular drugs.

## Experimental section

### Materials

*N*-Isopropylacrylamide (NIPAAm) and potassium persulfate (KPS) were purchased from Acros. Acrylic acid (AAc) (Merck) was redistilled *in vacuo* before use. α,α′-Azobisisobutyronitrile (AIBN) was used as received from Aldrich. 2-Aminoethanethiol hydrochloride (AET-HCl) and vinyl azlactone (VA) were obtained from TCI. All solvents, including methanol, methyl ethyl ketone (MEK), tetrahydrofuran (THF), dimethyl sulfoxide, and dicyclohexyl carbodiimide (DCC), were purchased from TEDIA. Other reagents, including potassium chloride (KCl), sodium chloride (NaCl), disodium hydrogen phosphate ($Na_2HPO_4$), and potassium phosphate monobasic ($KH_2PO_4$), were purchased from SHOWA, and deionized water with a resistivity of 18 MΩ cm was used throughout this work.

### Synthesis of the linear PAAc-*co*-PNIPPAm random copolymers

Linear PAAc-*co*-PNIPAAm was synthesized *via* free radical polymerization. The PNIPAAm network with ionizable groups was synthesized by the copolymerization of NIPAAm with different amounts of AAc; the required amount of AAc is shown in Table 1, and the synthetic scheme is given in Scheme 1a. In a two-neck flask, 44.25 mmol of NIPAAm and the required amount of AAc were dissolved in 90 mL of methanol. The polymerization was performed under a $N_2$ atmosphere by adding AIBN initiator at 60 °C and stirring for 20 h. The resultant copolymers were collected by precipitation in diethyl ether and dried in a vacuum oven.

### Synthesis of the PAAc-*g*-PNIPAAm graft copolymers

Amino-terminated oligomers of NIPAAm were synthesized *via* free radical polymerization of NIPAAm using AIBN and AET-HCl as the initiator and chain transfer agent, respectively. The reaction conditions are given in Table 1, and the synthetic route is shown in Scheme 1b. For the synthesis, 100 mmol of NIPAAm

Table 1 The preparation conditions and characterization of copolymers

| Polymers | AAc content (mmol) | NIPAAm content (mmol) | Macro NIPAAm content (g) | AIBN | $M_w$ | $M_n$ | PDI | AAc content (wt%) In feed | AAc content (wt%) In product |
|---|---|---|---|---|---|---|---|---|---|
| R*l*3[a] | 2.33 | 44.25 | | 1 mol% | 31 200 | 25 700 | 1.22 | 3 | 1.2 |
| R*l*5[a] | 3.33 | 44.25 | | 1 mol% | 29 900 | 24 800 | 1.21 | 5 | 3.2 |
| R*l*7[a] | 4.92 | 44.25 | | 1 mol% | 30 900 | 26 800 | 1.15 | 7 | 4.6 |
| G2*l*50[b] | 33.33 | | 2.4 | 0.333 mmol | 200 800 | 170 400 | 1.17 | 50 | 75.8 |
| G2*l*70[b] | 33.33 | | 1.03 | 0.333 mmol | 192 900 | 165 300 | 1.16 | 70 | 83.2 |
| G5*l*50[c] | 33.33 | | 2.4 | 0.333 mmol | 188 900 | 164 000 | 1.15 | 50 | 69.3 |
| G5*l*70[c] | 33.33 | | 1.03 | 0.333 mmol | 194 400 | 172 800 | 1.12 | 70 | 85.1 |

[a] Random copolymer prepared by free radical polymerization, 1 mol% of AIBN used as initiator to monomer. [b] Graft copolymer prepared from oligo-NIPAAm ($M_w = 2200$). [c] Graft copolymer prepared from oligo-NIPAAm ($M_w = 5000$).

monomer, 4 mmol of AET-HCl, and 1 mmol of AIBN were dissolved in 50 mL of methanol, followed by heating at 60 °C for 20 h in a $N_2$ atmosphere. After completion, the reaction product was precipitated into diethyl ether and dried in a vacuum oven. To prepare macromers of NIPAAm, ring-opening polymerization of VA was performed using amino-terminated oligo-NIPAAm as the initiator. First, 1.95 mmol of oligo-NIPAAm and 5.9 mmol of VA were dissolved in 100 mL of dry THF and reacted at 40 °C for 16 h in a $N_2$ atmosphere. The mixture was then poured into diethyl ether to precipitate the product, which was dried in a vacuum oven.

PNIPPAm chains grafted onto a PAAc backbone were prepared by AIBN-initiated copolymerization of the macromonomer of NIPPAm with different weight to volume (w/v) ratios of AAc at 60 °C for 2 h. To remove any unreacted macromonomer and AAc monomer, the reaction mixture was dropped into MEK and filtered. For further purification, the product was dissolved in methanol and precipitated by the addition of THF.

### Characterization

The polymerization intermediates and products were characterized using infrared spectroscopy and $^1$H NMR spectroscopy. The $^1$H NMR spectra were recorded on a Bruker Avance 500 MHz NMR spectrometer using $D_2O$ as a solvent. FT-IR spectra were recorded on a Nicolet 6700 (Thermo scientific) FT-IR spectrometer. The number average molecular weights of the copolymers ($M_n$) and polydispersity indices (PDIs; $M_w/M_n$) were determined by gel permeation chromatography using monodisperse polystyrene as the standard and dimethyl formamide (DMF) as the eluent at 30 °C. To understand the phase behavior of the copolymer, the phase transition was measured by dissolving the copolymer in phosphate buffer solution (PBS; 1 g $L^{-1}$, pH = 7.4) under UV light irradiation at 16–70 °C. The equilibrium water content of the linear polymer was measured gravimetrically: 0.1 g $mL^{-1}$ aqueous solutions were analyzed by immersion in a water bath at a constant temperature (34 °C) for 24 h. The film was separated from the solution, and filter paper was used to wipe the free water from the surface, after which the film was weighed. The water content of the copolymers was calculated as follows:

$$\%H_2O = \frac{\text{weight of wet sample} - \text{weight of dry sample}}{\text{weight of wet sample}}$$

### *In vitro* cytotoxicity

To understand the cytotoxicity of the PAAc-*co*-PNIPAAm, various concentrations (30–90 μg $mL^{-1}$) of PNIPAAm, copolymers, and their corresponding monomers were tested *in vitro* in 24 h cycles, using corneal tissue of New Zealand white rabbits. The experiments used an MTT assay according to previously reported methods to quantify cell viability and were carried out in triplicate.[29]

### Release of epinephrine from the copolymer films

To evaluate the drug release from the drug-loaded copolymer films, samples containing 10% w/v of random or graft copolymer were separately mixed with trace amounts of [$^3$H]-epinephrine as a model drug in PBS to form a polymer film and then held in an incubator at 34 °C. The physiology of the eye was simulated using 2.88 mL $h^{-1}$ of PBS instead of tears (*i.e.*, 40 times the physiological function), and the content of [$^3$H]-epinephrine in solution was measured every three minutes. To determine the release of [$^3$H]-epinephrine into the solution, an appropriate amount of Ecoscient™ H was added, and the solution was analyzed using a liquid scintillation analyzer (β-counter, TRI-CARB® 1500).

## Results and discussion

### Synthesis of the linear PAAc-*co*-PNIPAAm random copolymers

Two series of copolymers, *i.e.*, linear (PAAc-*co*-PNIPAAm) random copolymers and graft (PAAc-*g*-PNIPAAm) copolymers were synthesized by the free radical polymerization of NIPAAm with different amounts (wt%) of AAc monomer. The prepared random and graft copolymers have substantially different molecular structures despite having the same basic monomer structure, as shown in Scheme 1. The differences in the molecular structures of the resulting polymers were characterized by $^1$H NMR and FT-IR spectroscopy, as shown in Fig. 1 and 2, respectively. The $^1$H NMR spectrum contains peaks a and b (Fig. 1), which are attributed to the PNIPAAm segments with

 

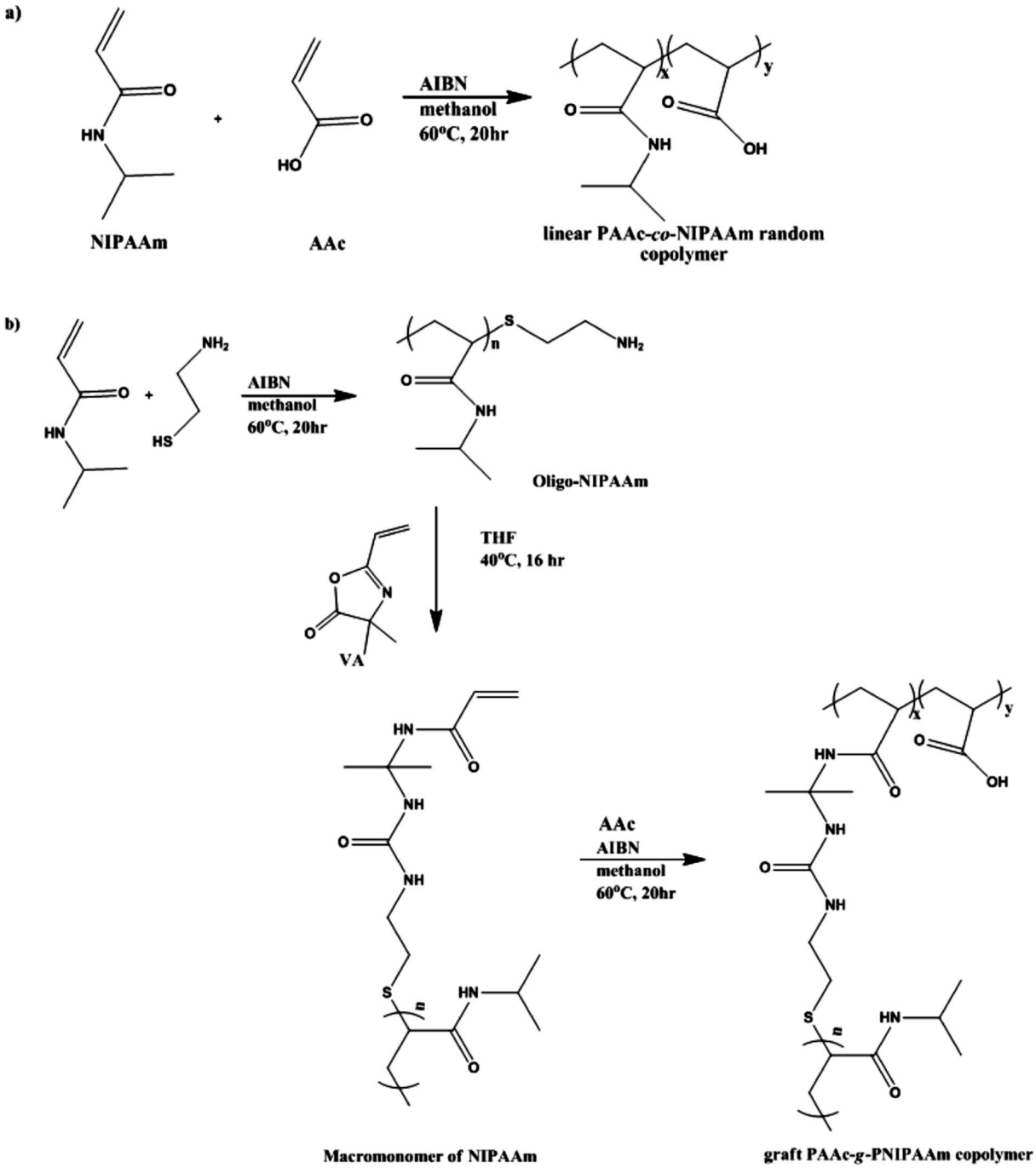


Scheme 1 Schematic representation of the synthesis of the (a) random copolymers and (b) graft copolymers.

additional contributions from the PAAc segments. Additionally, the peaks at 1.05 and 3.78 ppm correspond to the methyl ($-CH_3$) and methyne (–CH–) isopropyl hydrogen atoms, respectively, while the peaks at 1.22 and 1.91 ppm are assigned to the methylene and methyne protons of the main chains. The integration intensity of each segment was calculated based on the integral values of the main and side chain hydrogen values, which are attributed to the addition of PAAc into the PNIPAAm segments; the segment ratio of PAAc-*co*-PNIPAAm is shown in Table 1.

The FT-IR results confirmed the success of the free radical polymerization. As shown in Fig. 2, the FT-IR spectrum of PAAc-*co*-PNIPAAm differs from that of pure NIPAAm. The spectrum of the unreacted NIPAAm monomer exhibits a secondary amine stretching vibration at 3310 $cm^{-1}$ and a C=C absorption band at 1625 $cm^{-1}$. The characteristic peak at 1655 $cm^{-1}$ in the NIPAAm spectrum is attributed to amide stretching; this peak is also found at the same position in the FT-IR spectrum of the random copolymer, which features an additional peak at 1710 $cm^{-1}$ due to the carbonyl stretching of the acrylic acid

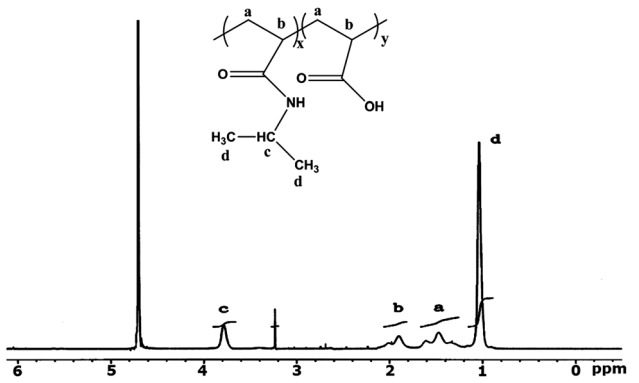


Fig. 1 $^1$H NMR spectra of the PAAc-*co*-PNIPAAm random copolymers.

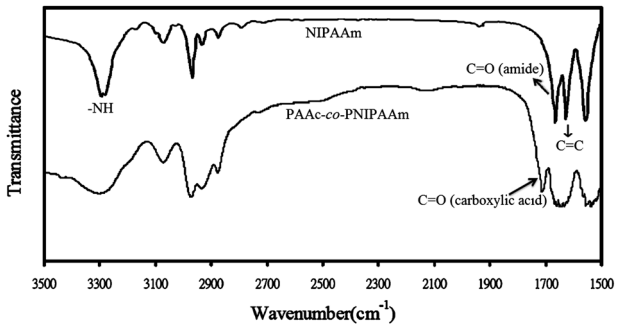


Fig. 2 FT-IR spectra of the PAAc-*co*-PNIPAAm random copolymers.

carboxyl groups of PAAc-*co*-PNIPAAm. The polymerization was confirmed by the absence of the C=C absorption bands at 1625 cm$^{-1}$ in the copolymer.

### PAAc-*g*-PNIPAAm graft copolymers

To prepare the graft copolymers, oligo-NIPAAm was first synthesized by attaching a chain transfer agent to NIPAAm; this reaction was confirmed by both FT-IR and $^1$H NMR spectroscopy (ESI, Fig. S1 and S2†). The formation of oligo-NIPAAm was confirmed by the broad peaks from 3300–3450 cm$^{-1}$, which are attributed to the $-NH_2$ stretching vibration, and the disappearance of the C=C vibration band at 1625 cm$^{-1}$. The $M_n$ and PDI values of the $NH_2$-terminated oligo-PNIPAAm were determined *via* GPC to be 1980 g mol$^{-1}$ and 1.16, respectively. Additionally, the $^1$H NMR spectrum of the oligo-NIPAAm features two main characteristic peaks at 2.72 and 3.09 ppm, which are attributed to the $NH_2$–$CH_2$–$CH_2$ and S–$CH_2$–$CH_2$ moieties, respectively.

Similarly, macromer-NIPAAm was prepared by the radical polymerization of oligo-NIPAAm using VA as a chain transfer agent. The $^1$H NMR spectrum of the NIPAAm macromonomer (ESI, Fig. S2†) shows two peaks at 5.62 and 6.1 ppm, which are attributed to the vinyl protons; this result confirms that the polymerizable end groups were introduced onto the NIPAAm backbone.

Graft copolymer PAAc-*g*-PNIPAAm was prepared *via* free radical polymerization and characterized by $^1$H NMR and FT-IR spectroscopy, as shown in Fig. 3 and 4, respectively. The absence of the peaks at 5.62 and 6.1 ppm corresponding to the vinyl protons, which appeared in the $^1$H NMR spectrum of the NIPAAm macromer, indicate that the vinyl end groups of the NIPAAm macromer were polymerized by AIBN. FT-IR spectroscopy was used to further verify the functional groups of the PAAc-*g*-PNIPPAm graft copolymer (Fig. 4). The FT-IR spectrum displays a broad band approximately 3330 cm$^{-1}$, which is attributed to –NH stretching vibrations, and a peak at 1645 cm$^{-1}$, which corresponds to the stretching of the C=O moiety of the amide. The introduction of the PAAc segments into the PAAc-*g*-PNIPPAm graft copolymer was confirmed by the appearance of an additional peak at 1720 cm$^{-1}$, which corresponds to the stretching of the C=O moiety of the carboxylic group; this result also supports the formation of the copolymers.

The molecular weights of the random and graft copolymers were measured using GPC in DMF as the solvent medium and are shown in Table 1. Both the random and graft copolymers prepared with different amounts of AAc exhibit a similar molecular weight and polydispersity index (PDI). However, the

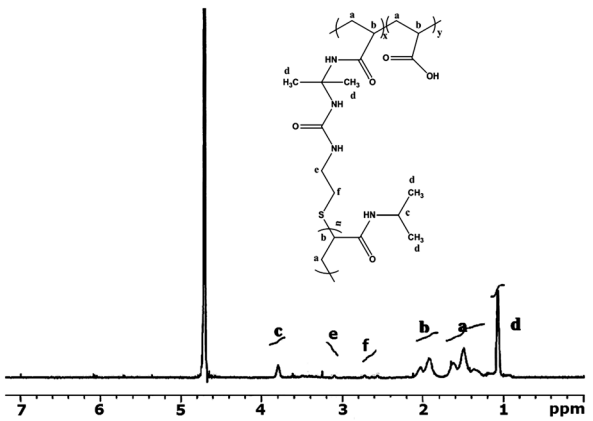


Fig. 3 $^1$H NMR spectra of the PAAc-*g*-PNIPPAm graft copolymers.

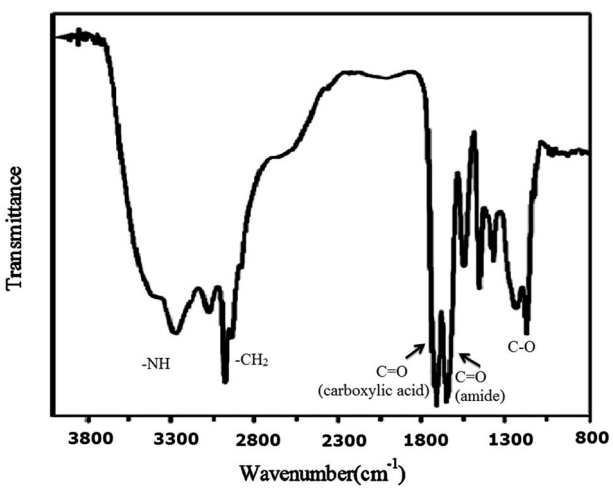


Fig. 4 FT-IR spectra of the PAAc-*g*-PNIPPAm graft copolymers.

graft copolymer has a significantly lower molecular weight than the random copolymer; this is due to the lower polymerization reactivity of PAAc, which is a result of the steric hindrance of the chain during chain propagation.

### Phase transition behavior of the copolymers

As expected, both the random and graft copolymers exhibited thermoresponsive properties because the copolymer backbones contain thermally sensitive segments. The phase transition properties of the random and graft copolymers were measured using the cloud point method, which involves monitoring the optical absorbance of the polymer solution as a function of the temperature; the results for the random and graft copolymers are shown in Fig. 5a and b, respectively. The LCSTs of the linear PAA-*co*-PNIPAAm random copolymers in PBS (pH 7.4) were ~46, 52, and 58 °C for R*l*3, R*l*5, and R*l*7, respectively. The LCST of the random PAAc-*co*-PNIPAAm increases rapidly with increasing acrylic acid content at pH 7.4 because acrylic acid is more hydrophilic than NIPAAm in both its protonated and deprotonated states. However, the LCSTs of the graft PAAc-*g*-PNIPAAm copolymers were fairly constant at ~34 °C with increasing acrylic acid content at pH 7.4, which is almost the same as that of pure PNIPAAm. Illustrations of the possible phase separations are shown in Scheme 2a. In general, changes in the hydrophilic/hydrophobic balance of the polymer can affect the phase transition of the PNIPAAm-based polymers. Thus, the hydrophilic/hydrophobic balance of PAAc-*co*-PNIPAAm in aqueous solution was altered through the hydrogen bonding interactions between the water molecules and the PAAc segments. Water molecules interact more strongly with PAAc segments than with PNIPAAm, which is due to the increased content of hydrophilic AAc. The random copolymer could be ionized to a greater extent at pH 7.4, and the hydrogen bonding interactions between the water molecules and polar groups of PAAc may improve the solubility as more solvent molecules interact with the polar PAAc segments.[30] Additionally, the polymer chains extend due to the electrostatic repulsion between the charged groups along the polymer backbone, which reduces the polymer–polymer interactions. Accordingly, the LCST of the random copolymer increases with increasing PAAc content at pH 7.4. In contrast, the graft copolymers slightly extend due to the electrostatic repulsion between the charged groups along the polymer because the polymer chains are cross-linked. Eventually, inter- and intra-molecular hydrogen bonds form between polymer chains, which may interfere with the access of water molecules to the amide groups of the PNIPAAm; as a result, the graft PAAc-*g*-PNIPAAm copolymer chains become more hydrophobic. Due to the limited accessibility of water molecules from the nearby water clusters, the hydrophobic isopropyl groups may facilitate the hydrophobic interactions between polymers, resulting in polymer precipitation, which leads to the LCST of the graft PAAc-*g*-PNIPAAm polymers being similar to that of pure PNIPAAm.

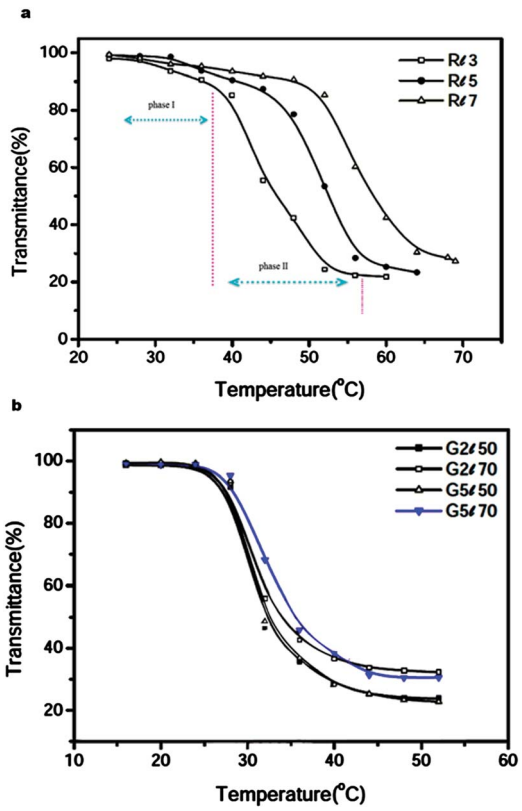


Fig. 5 Phase transition behavior of the copolymers as a function of temperature in buffer solutions at pH 7.4: (a) random copolymer and (b) graft copolymer.

### Equilibrium water content

To evaluate their equilibrium water content, the graft PAAc-*g*-PNIPAAm copolymers were assessed as films at 34 °C; the results are shown in Fig. 6. Since the linear PAAc-*co*-PNIPAAm random copolymers, such as R*l*5 and R*l*7, have LCSTs that are too high and failed to form polymer films at 34 °C, the water content of these polymers could not be determined, and an *in vitro* simulation of drug release from the film could not be performed. However, two types of phase transition temperatures are evident for the R*l*3 random copolymer, and the lower temperature region of the phase transition temperature is used to form a film at 34 °C. Due to the limited volume of film formed, the water content of this copolymer is lower than that of the graft copolymers. The water content of the graft PAAc-*g*-PNIPAAm copolymers increased with increasing AAc content; for example, the copolymer containing 70 wt% AAc has a higher water content than that containing 50 wt% AAc, which clearly shows that the hydrophilic nature of AAc enhances the adsorption of water to the polymer chains. Moreover, PAAc with higher molecular weight PNIPAAm side chains has a higher water content than that with lower molecular weight PNIPAAm side chains because water molecules become entrapped between the side chains. Fig. 6 shows that the higher molecular weight PNIPAAm side chains form intermolecular hydrogen bonds between polar groups and subsequently form aggregates of PNIPAAm chain segments; accordingly, these entanglements may trap water, leading to the observed higher water content (Scheme 2b).

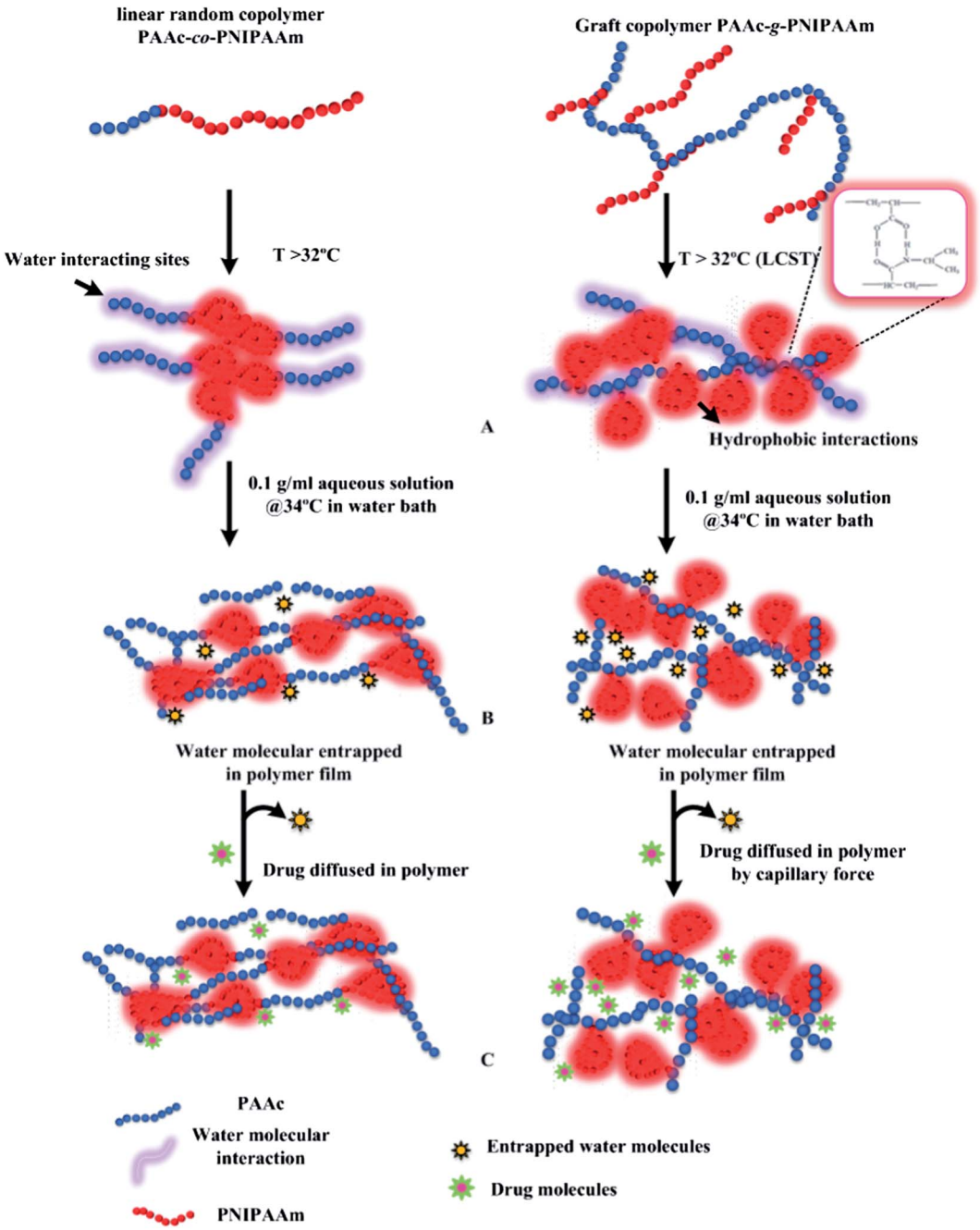


Scheme 2 Schematic illustration of the (a) phase transition behavior, (b) water adsorption behavior, and (c) drug diffusion behavior of the copolymers.

### *In vitro* cytotoxicity and drug delivery

To estimate the biocompatibility of the copolymers, *in vitro* cytotoxicity experiments were performed for both the random and graft PAAc-*co*-PNIPAAm copolymers and are shown in Fig. 7. Both monomers exhibited significant cytotoxicity, and PNIPAAm induced a slight cytotoxic response at higher concentrations. Interestingly, both copolymers demonstrated no apparent cytotoxicity, *i.e.*, the growth rate of the cultured corneal cells was not inhibited by the copolymers due to their hydrophilic surface at the observed temperature. The polymers with a hydrophilic corona do not interfere with the cell membranes resulting in an almost non-cytotoxicity. By comparison with our previous report, a drug carrier constructed with pure PNIPAAm is difficult to modulate by temperature changes under physiological conditions because the physiological temperature is higher than the phase transition temperature of pure PNIPAAm.[13] In particular, the corneal temperature is approximately 34 °C, and its temperature range is narrow.[31,32] In general, the phase transition temperature of PNIPAAm can be easily tuned by the addition of AAc as a comonomer. It was found that the phase transition temperature

 

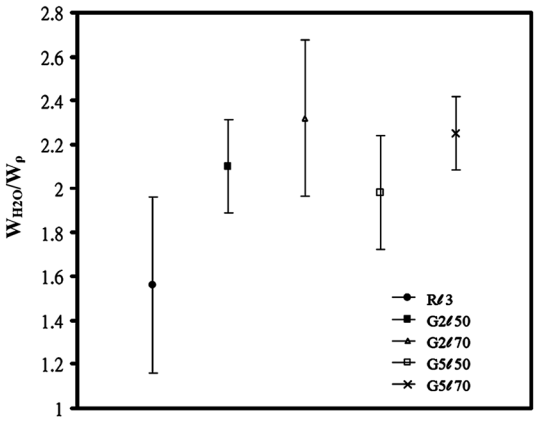


Fig. 6 Equilibrium water content of the copolymer films.

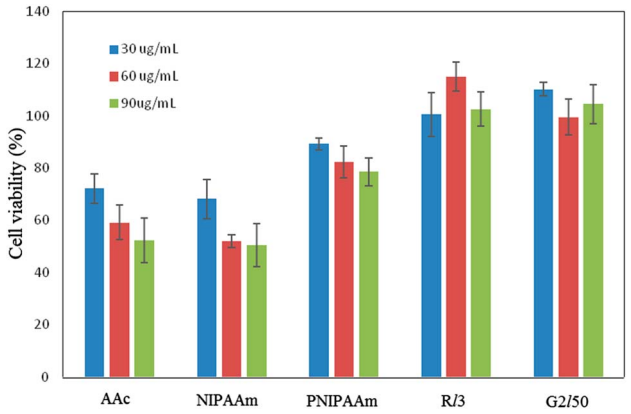


Fig. 7 Cell viability of the copolymers or monomers after 24 h incubation. The MTT assay was carried out using corneal tissue of New Zealand white rabbits.

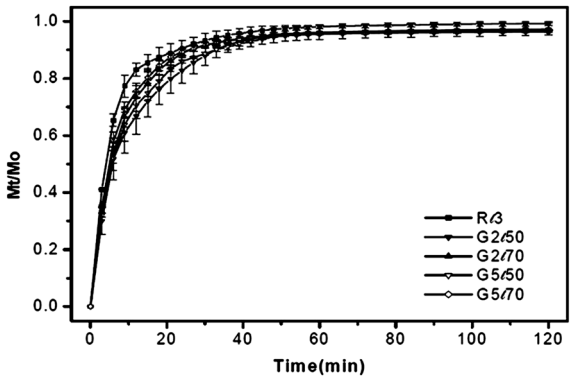


Fig. 8 [$^3$H]-Epinephrine release as a function of time from the copolymer films.

could be adjusted to 34 °C by the incorporation of PAAc into the PNIPAAm chains, which is almost equal to the corneal surface temperature. Moreover, the NIPAAm homopolymer became a rigid, uncomfortable film after coming into contact with the cornea.[13] Hence, the film formation of the graft PAAc-*g*-PNIPAAm copolymers is hastened compared to the random PAAc-*co*-PNIPAAm copolymers at 34 °C, due to their phase transition temperature. Such a film-forming behavior can facilitate the application of eye drops in ophthalmic drug delivery with controlled release.

[$^3$H]-Epinephrine is a well-known drug used to reduce the IOP in glaucoma therapy; it affects the main parameters of aqueous humor dynamics such as aqueous production and trabecular outflow, which may serve as moderators for changes in intraocular pressure. Therefore, a graft copolymer loaded with [$^3$H]-epinephrine was prepared for controlled ophthalmic drug delivery applications; the release profile at pH 7.4 is shown in Fig. 8. The time-dependent drug release was recorded for all formulations, and the release tendencies of all the copolymers were similar. However, there is a slight variation in the release profile of the linear PAAc-*co*-PNIPAAm random copolymer, which is related to the water content of the copolymers. Random copolymer R*l*3 contains less water than the graft copolymers, which results in faster drug release. Accordingly, graft copolymers with higher water contents, such as G2*l*70 and G5*l*70, demonstrate more sustained release. Thus, a higher water content in the copolymers results in the formation of a larger capillary network in the polymer matrix, which promotes drug diffusion into the copolymer, as shown in Scheme 2c. An efficient drug delivery system should have a high loading capacity and enable sustained release of the drug; the synthesized graft PAAc-*g*-PNIPAAm copolymers should be ideal for sustained release due to their film-forming behavior, which can overcome the rigid film formation on the surface of the cornea, as demonstrated in an animal study (ESI, S3†). Lower IOP was observed after administration of the polymeric eye-drops ([$^3$H]-epinephrine contains graft PAAc-*g*-PNIPAAm copolymers) on a rabbit, which suggests that the synthesized graft PAAc-*g*-PNIPAAm copolymers in the eye drops had a beneficial effect on the sustained delivery. However, more detailed investigations are required to elaborate and are currently in progress.

One of the main objectives of this study is to reveal the release mechanism of a model drug from the synthesized copolymers. To evaluate the drug release mechanism of the drug-loaded graft copolymers, a theoretical model must be applied to elucidate the release kinetics. Because drug delivery is quite complex, the theoretical models are fitted with experimental data when the release profiles depend on single or multiple mechanisms. In general, such a theoretical model was mainly developed to predict the release of drugs from polymeric materials with various shapes, such as spheres, cylinders, discs, or slabs. The following semi-empirical equation (*i.e.*, Ritger–Peppas model)[33] was used to fit our experimental data to determine the release kinetics (*i.e.*, Fickian or non-Fickian):

$$\frac{M_t}{M_0} = kt^n \quad (1)$$

where $M_t$ and $M_0$ are the cumulative amount of drug released at time $t$ and the total amount of drug loaded into the system, respectively, $k$ is the diffusion kinetic constant of the drug–polymer system, and $n$ is the diffusion exponent of the drug release mechanism. Based on the above assessment of the release kinetics from a swollen slab-like geometry (*i.e.*, thin

film), the release exponent values indicate the following: when $n = 0.5$, the mechanism is purely Fickian diffusion; when $0.5 < n < 1.0$, the release is anomalous (*i.e.*, non-Fickian); when $n = 1$, the mechanism is Case II dominant transport, in which the drug release from the thin film is zero order and independent of the time; and when $n > 1$, the mechanism involves super Case II transport of the drug. Case II transport involves relaxation of the macromolecules due to the movement of water into the system, which is considered to be the rate-controlling step. The results from the drug release experiments were fitted by the Ritger–Peppas model, which is based on Fickian diffusion during drug release; the resultant kinetic constants and diffusion coefficients are listed in Table 2. The value of $n$ was found to be between 0.5 and 0.6, which indicates that the drug transport mechanism was anomalous (*i.e.*, non-Fickian diffusion); this involves both diffusion and polymer relaxation during the release profile.[34]

A theoretical model of the entire drug release process is quite complicated due to the many parameters that must be accounted for, such as drug diffusion from the device, water entering the device, electrostatic interactions between the polymers and the drug, ionic strength, and concentration. With these assumptions, the applicability of particular models could be limited to particular polymer–drug systems. Interestingly, our systems are best described by the Peppas ($0.5 < n < 0.6$) model. The release profile and the fitting of the experimental results to theoretical models are shown in Fig. 9. Grafted polymer G2*l*50 shows a lower $k$ value than the linear copolymer with the same PAAc content. However, the other grafted copolymers show higher $k$ values due to the presence of PNIPAAm in the side chains, which easily forms strong intermolecular interactions between the polymer chains, thereby accelerating polymer chain shrinkage and extrusion of the drug from the polymer matrix. The lowest $k$ value indicates that the rate of release from this matrix is significantly slower than that from the polymer matrices. All the kinetic data show a very good fit with eqn (1), as denoted by the values of $R^2$ (>0.96).

Table 2 The *in vitro* release kinetic parameters of different copolymers

| Copolymer | $N$ | $k$ | $R^2$ |
|---|---|---|---|
| R*l*3 | 0.5191 | 0.2412 | 0.969 |
| G2*l*50 | 0.5832 | 0.1663 | 0.9633 |
| G2*l*70 | 0.5749 | 0.1837 | 0.9852 |
| G5*l*50 | 0.5793 | 0.1747 | 0.9842 |
| G5*l*70 | 0.5679 | 0.1944 | 0.9716 |

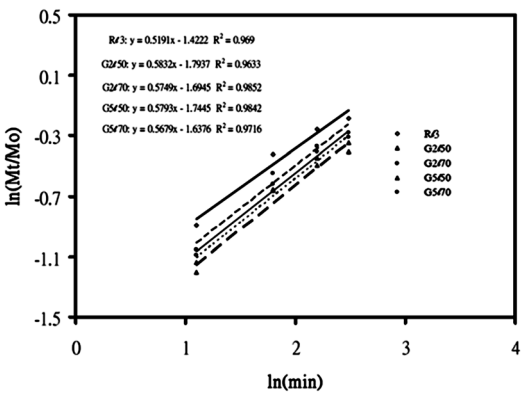


Fig. 9 The *in vitro* drug release parameters of the different copolymers fitted by the Ritger–Peppas model.

## Conclusions

An effective polymeric carrier for ophthalmic drug delivery was obtained *via* copolymerization of PAAc and PNIPAAm; the resultant copolymer could successfully modulate the release of [$^3$H]-epinephrine. A straightforward synthetic strategy based on random and graft copolymerization was used for the synthesis of the random and graft copolymers. The random linear copolymer showed a strong increase in LCST behavior above the physiological acceptable temperature due to the inclusion of AAc as a comonomer. In contrast, the graft copolymer showed a slight increase in the LCST at 34 °C. Moreover, the water content of the graft copolymers not only could be raised with increasing AAc content but also played a significant role in the drug release: the graft copolymer with a higher water content showed sustained release. The drug release followed a non-Fickian transport mechanism involving both diffusion and polymer relaxation during the release. The proposed thermoresponsive copolymers could be effective as topical ophthalmic drops for glaucoma therapy.

## Acknowledgements

We are indebted to Department of Health of the Republic of China, Taiwan for financially supporting this work with National Research Program for Biopharmaceuticals (DOH101-TD-PB-111-TM011/ 101TM007), National Science Council of the Republic of China, Taiwan, for financial support (102-2811-P-033-001, 103-2811-E-033-001 and 102-2221-E-033-011).

## References

1 M. D. David Fleischman and M. D. R. Rand Allingham, *Saudi J. Ophthalmol.*, 2013, **27**, 97.
2 Y. Kapoor and A. Chauhan, *Int. J. Pharm.*, 2008, **361**, 222.
3 M. Annaka, K. Mortensen, M. E. Vigild, T. Matsuura, S. Tsuji, T. Ueda and H. Tsujinaka, *Biomacromolecules*, 2011, **12**, 4011.
4 I. D. Rupenthal, R. G. Alany and C. R. Green, *Mol. Pharmaceutics*, 2011, **8**, 2282.
5 D. Schmaljohann, *Adv. Drug Delivery Rev.*, 2006, **58**, 1655.
6 S. H. Hu, S. Y. Chen, D. M. Liu and C. S. Hsiao, *Adv. Mater.*, 2008, **20**, 2690.
7 M. Patenaude and T. Hoare, *Biomacromolecules*, 2012, **13**, 369.
8 L. M. Bowman, E. Si, J. Pang, R. Archibald and M. Friedlaender, *J. Ocul. Pharmacol. Ther.*, 2009, **25**, 133.
9 M. Elsabahy and K. L. Wooley, *Chem. Soc. Rev.*, 2012, **41**, 2545.

 

10 A. S. Hoffman, *Adv. Drug Delivery Rev.*, 2013, **65**, 10.
11 E. Fleige, M. A. Quadir and R. Haag, *Adv. Drug Delivery Rev.*, 2012, **64**, 866.
12 Y. Wang, J. D. Byrne, M. E. Napier and J. M. DeSimone, *Adv. Drug Delivery Rev.*, 2012, **64**, 1021.
13 G. H. Hsiue, S. H. Hsu, C. C. Yang, S. H. Lee and I. K. Yang, *Biomaterials*, 2002, **23**, 457.
14 H. J. Jung and A. Chauhan, *Biomaterials*, 2012, **33**, 2289.
15 Z. M. O. Rzaev, S. Dincer and E. Piskin, *Prog. Polym. Sci.*, 2007, **32**, 534.
16 K. Haraguchi, T. Takehisa and M. Ebato, *Biomacromolecules*, 2006, **7**, 3267.
17 T. R. Hoare and D. S. Kohane, *Polymer*, 2008, **49**, 1993.
18 I. Dimitrov, B. Trzebicka, A. H. E. Mueller, A. Dworak and C. B. Tsvetanov, *Prog. Polym. Sci.*, 2007, **32**, 1275.
19 Y. Y. Liu, Y. H. Shao and J. Lu, *Biomaterials*, 2006, **27**, 4016.
20 L. G. Chen, Z. L. Liu and R. X. Zhuo, *Polymer*, 2005, **46**, 6274.
21 Y. Onuki, M. Nishikawa, M. Morishita and K. Takayama, *Int. J. Pharm.*, 2008, **349**, 47.
22 A. J. Winfield, D. Jessiman, A. Williams and L. Esakowitz, *Br. J. Ophthalmol.*, 1990, **74**, 477.
23 Y. Guan and Y. Zhang, *Soft Matter*, 2011, **7**, 6375.
24 J. Y. Lai and A. C. Hsieh, *Biomaterials*, 2012, **33**, 2372.
25 G. P. Misra, R. S. J. Singh, T. S. Aleman, S. G. Jacobson, T. W. Gardner and T. L. Lowe, *Biomaterials*, 2009, **30**, 6541.
26 S. B. Turturro, M. J. Guthrie, A. A. Appel, P. W. Drapala, E. M. Brey, V. H. Pérez-Luna, W. F. Mieler and J. J. Kang-Mieler, *Biomaterials*, 2011, **32**, 3620.
27 Y. Cao, C. Zhang, W. Shen, Z. Cheng, L. Yu and Q. Ping, *J. Controlled Release*, 2007, **120**, 186.
28 N. Pfeiffer, J. Lamparter, A. Gericke, F. H. Grus, E. M. Hoffmann and J. Wahl, *Cell Tissue Res.*, 2013, **353**, 245.
29 H.-C. Tsai, W.-H. Chang, C.-L. Lo, C.-H. Tsai, C.-H. Chang, T.-W. Ou, T.-C. Yen and G.-H. Hsiue, *Biomaterials*, 2010, **31**, 2293.
30 X. Yin, A. S. Hoffman and P. S. Stayton, *Biomacromolecules*, 2006, **7**, 1381.
31 H. Fujishima, I. Toda, M. Yamada, N. Sato and K. Tsubota, *Br. J. Ophthalmol.*, 1996, **80**, 29.
32 L. Kessel, L. Johnson, H. Arvidsson and M. Larsen, *Invest. Ophthalmol. Visual Sci.*, 2010, **51**, 6593.
33 P. L. Ritger and N. A. Peppas, *J. Controlled Release*, 1987, **5**, 23.
34 M. Curcio, I. Altimari, U. G. Spizzirri, G. Cirillo, O. Vittorio, F. Puoci, N. Picci and F. Iemma, *J. Nanopart. Res.*, 2013, **15**, 1581.